

# Classification of non-manifold singularities from transformations of 2-manifolds

J-C. Léon<sup>1</sup>, L. De Floriani<sup>2</sup>, F. Hétry<sup>3</sup>

<sup>1</sup>Grenoble University, CNRS, Laboratoire G-SCOP, 46 av. Félix Viallet, 38000 Grenoble, France

<sup>2</sup>University of Genova, Department of Computer Science, Via Dodecaneso, 35, 16129 Genova, Italy

<sup>3</sup>Grenoble University, CNRS and INRIA, Laboratoire Jean Kuntzmann, 655 av. de l'Europe, 38334 Montbonnot, France

**Abstract**—Non-manifold models are frequently encountered in engineering simulations and design as well as in computer graphics. However, these models lack shape characterization for modelling and searching purposes. Topological properties act as a kernel for deriving key features of objects. Here we propose a classification for the non-manifold singularities of non-manifold objects through continuous shape transformations of 2-manifolds without boundary up to the creation of non-manifold singularities. As a result, the non-manifold objects thus created can be categorized and contribute to the definition of a general purpose taxonomy for non-manifold shapes.

**Keywords**—non-manifold models; shape features; topology; simplicial complexes

## 1. INTRODUCTION

Non-manifold models are widespread to describe shapes in engineering applications as well as in cultural heritage, medicine, etc. Usually, such models express a local or global abstraction or idealization of the digital shape of an object with regard to its physical shape, which is volume-based [1], [2]. However, it is still difficult to characterize such shapes on a global basis to be able to identify through holes or handles or even some other features that can be useful in many applications. These shape properties can be subdivided into application-dependent ones and generic ones. Here, the focus is placed on generic ones.

Non-manifold models have been introduced in geometric modelling long time ago [3], [4]. Early works have concentrated on the local characterization of non-manifold models for boundary modeling, and such characterization has considered the neighbourhood of vertices and edges to distinguish manifold configurations of curves and surfaces from the non-manifold ones. These contributions refer to local topological properties. Few contributions [5], [6] focused on the connection between shape global properties and non-manifold configurations based on global topological parameters. Contrary to the previous ones, these contributions refer to global topological properties and especially the Euler-Poincaré theorem [7].

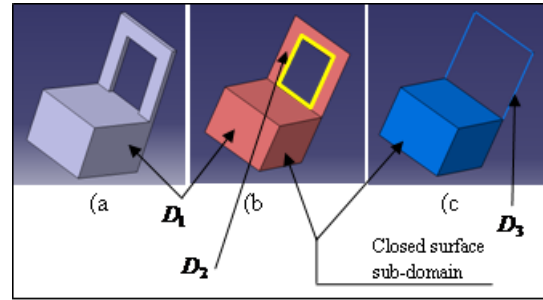


Fig. 1. Concept of hole and handle as seen through a shape idealization process: (a) the initial volume object, (b) the same object after idealizing the top part of the volume into a surface with boundary, thus producing a non-manifold object with two components  $D_1$  and  $D_2$ , (c) the same object after idealizing  $D_2$  into  $D_3$ .

For a general purpose taxonomy of non-manifold objects, topological aspects are addressed to distinguish classes of objects. Presently, it is restricted to categories of non-manifold objects generated from reference shapes used in combinatorial topology, i.e., sphere, torus, Klein bottle, projective plane. This is a way to classify non-manifold singularities derived from 2-manifolds without boundary. Here, the transformations of the reference shapes into non-manifold objects cover various connections between what we call *manifold connected components* [8], forming the object. Their key features are highlighted to show how they distinguish from each other.

## 2. MOTIVATION

The contribution addresses a general purpose shape classification of non-manifold 3D objects embedded in the Euclidean space  $E^3$ . It complements a first proposal [9] covering non-manifold singularities generated from orientable 2-manifolds with or without boundaries.

A 2-manifold embedded in  $E^3$  stands as a reference concept where topological properties for shape classification is well established. The resulting classification is a contribution to search and retrieval functions of non-manifold 3D objects. The non-manifold singularity classification is also a basis of modelling functions for non-manifold 3D objects to better match the shape diversity needed for a given application involving a modelling process.

As a general requirement, global topological properties of non-manifold objects contribute to the definition of shape features. Among them, holes or handles are of particular interest to a general taxonomy. As an example illustrating the interaction between global topological properties, shape features like handles and non-manifold models are shown in Figure 1. Here, three objects are depicted sharing a common shape feature (a handle), where Figure 1b and c are non-manifold models. Characterizing such configurations motivates the proposed classification presently reduced to non-manifold configurations derived from 2-manifolds without boundary.

### 3. BACKGROUND

Here, we consider a discretization for non-manifold objects embedded in the three-dimensional Euclidean space  $E^3$  as simplicial 2-complexes [7], [8]. These objects differ from CAD models but they are considered as a first step in the current work for simplicity. For a simplicial 2-complex  $\Sigma$ , a global topological invariant is defined by the Euler-Poincaré formula:

$$v - e + f = \beta_0 - \beta_1 + \beta_2, \quad (1)$$

where  $v$ ,  $e$  and  $f$  are the number of vertices, edges and faces, respectively, of  $\Sigma$ .  $\beta_0$ ,  $\beta_1$ ,  $\beta_2$ , are the Betti numbers which denote the number of connected components, 1-cycles and 2-cycles, respectively.

We can characterize the non-manifold singularities of a simplicial complex by considering the neighborhood of vertices and edges defined through the concepts of star and link [10].

In order to analyze a non-manifold object, we consider a decomposition of its simplicial representation into *manifold-connected* components as defined in [8]. Hence, a manifold-connected 2-complex may contain both non-manifold vertices and edges.

Intuitively, a decomposition  $\Delta$  of a complex  $\Sigma$  is a collection of sub-complexes of  $\Sigma$ , such that the union of the components in  $\Delta$  is  $\Sigma$ , and any two components  $\Sigma_1$  and  $\Sigma_2$  in  $\Delta$ , if they intersect, intersect at a collection of non-manifold vertices and edges. Intuitively, an *MC-decomposition* is constructively defined by cutting a complex  $\Sigma$  only at all its non-manifold vertices and edges and forming components that satisfy the following property: two  $k$ -dimensional top-simplexes  $\sigma_1$  and  $\sigma_2$  belong to the same component in the MC-decomposition if and only if there exists a manifold  $(k-1)$ -path that connects  $\sigma_1$  and  $\sigma_2$  in  $\Sigma$ .

Indeed, non-manifold singularities act as new configurations and need to be characterized topologically. Here, transformations of 1-cycles over 2-manifolds are particularly under focus.

### 4. NON-MANIFOLD SINGULARITIES AND CONNECTIONS AMONG MC-COMPONENTS

In this section, we discuss non-manifold singularities and non-manifold connections among MC-components, and then we introduce definitions about self-intersections.

First of all, MC-components may contain singularities in the form of non-manifold vertices and edges, that we call *intrinsic*. A vertex and/or an edge inside an MC-component  $D_i$  is called an *intrinsic* singularity when it is a non-manifold vertex or edge for  $D_i$  considered as a standalone object. The connected components of the non-manifold intrinsic singularities of a component  $D_i$  form a simplicial 1-complex not containing 1-cycles.

*External singularities* in an MC-component  $D_i$  are those edges or vertices in  $D_i$  which are non-manifold edges and vertices, respectively, in the original complex  $\Sigma$  and are shared by  $D_i$  and at least another MC-component. Note that an intrinsic singularity can be an external one as well.

In order to address a wide range of shapes, orientable and non-orientable 2-manifolds, respectively embedded and immersed in  $E^3$  are considered. Classical non-orientable surfaces like the Klein bottle and the projective plane immersed in  $E^3$  are self-intersecting. Here, the purpose is to highlight the concept of self-intersection in the context of non-manifold objects, hence the introduction of *implicit* and *explicit* self-intersections.

$S_I$  is a *self-intersecting 2-manifold* embedded in  $E^3$ , described with a parametric mapping:

$$\begin{aligned} M_p : (u_1, u_2) &\mapsto (x(u_1, u_2), y(u_1, u_2), z(u_1, u_2)) \\ &= P(u_1, u_2), \end{aligned}$$

if there exists at least two points  $P_1$  and  $P_2$  of  $S_I$  satisfying the following equation:

$$\begin{aligned} P_1(u_{11}, u_{12}) &= P_2(u_{21}, u_{22}) \\ \text{where } (u_{11}, u_{12}) &\neq (u_{21}, u_{22}). \end{aligned}$$

An *implicit self-intersection* of a MC-component  $D_j$ , of dimension 2, is such that the self-intersection points  $P_i$  of  $D_j$  have no associated topological entity in  $D_j$ . As a result, the self-intersections are defined strictly geometrically because no topological entity takes part to their description. This configuration is representative of the combinatorial topology used to define the topological invariant of 2-manifold objects [7].

An *explicit self-intersection* of an MC-component  $D_j$  of dimension 2, is such that all its self-intersection points  $P_i$  are associated either to 0-simplexes  $\sigma_{0k}$  or to 1-simplexes  $\sigma_{1k}$  of  $D_j$  depending on the configurations of self-intersections existing in  $D_j$ . Let  $\Omega_0$  be the subset of points  $P_i$  associated to 0-simplexes of  $D_j$ , i.e.,  $\forall P_i \in \Omega_0, \exists \sigma_{0k} \in \Sigma$  such that  $P_i \mapsto \sigma_{0k}$ . Similarly, let  $\Omega_1$  be the subset of points  $P_i$  associated to 1-simplexes of  $D_j$ , i.e.,  $P_i$  contains sets of points  $P_{1kt}$  forming lines  $L_k$  of  $D_j$ ,  $L_k = \bigcup_t P_{1kt}$ , then:

- $\forall L_k \in \Omega_1, \exists \sigma_{1h} \in \Sigma$  such that  $L_k \mapsto \sigma_{1h}$ ,
- $\forall (L_\alpha, L_\beta)$  with  $L_\alpha \cap L_\beta = P_i, P_i \in \Omega_0$ ,
- $(\Omega_0 \cup \Omega_1) = \bigcup_i P_i$ ,
- $((\bigcup_k \sigma_{0k}) \cup (\bigcup_h \sigma_{1h})) \subset \Sigma$ .

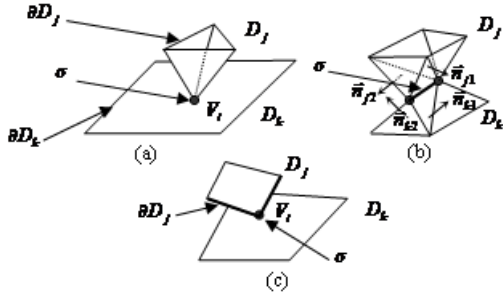


Fig. 2. a) An example of non-manifold connection between two MC-components  $D_j$  and  $D_k$  at a 0-simplex, b) connection between  $D_j$  and  $D_k$  at a 1-simplex and characterization of  $\Theta$  with transition information, c) connection where  $D_k$  is a MC-component with boundary.

When restricting the consideration to manifold shapes as it happens in combinatorial topology [7], explicit self-intersections cannot occur because such configurations would produce non-manifold configurations, which are contradictory to the concept of manifold required to state the properties derived from combinatorial topology. Here, self-intersecting surfaces like the Klein bottle will be addressed as non-manifold configurations and hence, they will be described with explicit self-intersections.

In order to characterize the orientation properties of non-manifold objects, the orientation of each MC-component must be taken into account and combined with the others to characterize the embedding or the immersion of these objects. More precisely, the orientation of the MC-components  $D_j, D_k, \dots$ , in the neighbourhood of each non-manifold connection of  $\Sigma$  can be described in a combinatorial manner using a function  $\Theta$ .  $\Theta$  is called the *transition function* across MC-components  $D_j$  and is obtained from properties of the embedding of  $\Sigma$ . For example, parameterization properties can be used to define  $\Theta$  over  $\Sigma$  and help characterizing a Klein bottle as a specific category of cellular decomposition (see section V).

**Property.** *Transition function at a 0-simplex*

Let  $D_j$  and  $D_k$  be two MC-components of  $\Sigma$ , connected together such that their non-manifold connection occurs at a 0-simplex, i.e.,  $D_j \cap D_k = \sigma$  where  $\sigma$  is a 0-simplex (see Figure 2a). If  $D_j$  and  $D_k$  are both MC-components without boundary,  $\sigma$  is the apex of a cone at least in  $D_j$  or  $D_k$ . Therefore, there is no normal defined at  $\sigma$  for at least one MC-component and no orientation information can be assigned to the transition between  $D_j$  and  $D_k$  to characterize it. Similarly, if  $D_j$  is a MC-component without boundary and  $D_k$  a MC-component with boundary or the opposite or if both are MC-components with boundaries, and  $D_j$  and  $D_k$  are connected together at  $\sigma$ , a 0-simplex,  $\sigma$  is also the apex of a cone for  $\partial D_j$  (or  $\partial D_k$ ), hence no transition information can be assigned to this configuration too.

As a consequence,  $\Theta$  is meaningful when a non-manifold connection contains at least one 1-simplex.

This property is also applicable to a single MC-component containing a non-manifold singularity. Figures 2a and b illustrate two configurations where the non-manifold connections contain a 0-simplex and a 1-simplex respectively. Figure 2c is an example of non-manifold connection where  $D_j$  is connected through its boundary.

Details about the description of  $\Theta$  and the connection between MC-components require more developments and could not fit into this paper.

## 5. CLASSIFICATION OF MC-DECOMPOSITIONS WITH NON-MANIFOLD SINGULARITIES

Here, we consider objects discretized as simplicial complexes with non-manifold singularities, but such that each complex defines a single object, i.e., only one immersion or embedding is defined. This category is also combined with different types of connections between MC-components, i.e., either intrinsic or external and, in any case the self-intersecting objects are analyzed through their explicit self-intersections.

Our taxonomy is based on degenerated configurations of the basic surfaces used in classical combinatorial topology (sphere, torus, projective plane and Klein bottle).

In the following examples, it should be noticed that the shapes are modelled as smooth surfaces rather than simplicial complexes to simplify their graphics representations.

### 5.1 Degenerate spheres

Let us take a topological sphere embedded in  $E^3$  as initial configuration. Non-manifold singularities can be created using the *pinching* operator, which continuously deforms the sphere until two different points are merged. This operator can be used once or several times, leading to the following non-manifold configurations:

- sphere *pinched* at a point with two possible orientations,
- sphere *pinched* several times at the same point introducing the concept of arity of pinched configuration,
- sphere *pinched* along a line generating two classes of objects:
  - a sphere as a real volume object ; a non-manifold object embedded in  $E^3$ ,
  - or an object like a cross cap ; a non-orientable object immersed in  $E^3$ ,

illustrating the impact of the transition function  $\Theta$  to characterize the possible orientations around the *pinched* connection,

- along a non-manifold configuration with or without closed lines.

In the first case, the number of vertices  $v$ , decreases by one,  $e, f, \beta_0, \beta_2$  stay unchanged. Therefore, according to eq. (1),  $\beta_1$  must increase by one. The key feature characterizing the *pinched* configuration is the

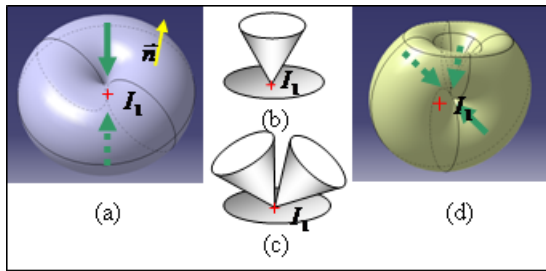


Fig. 3. Examples of neighbourhoods of connections at a vertex  $I_1$  intrinsic to  $D_j$ : (b) case of two disks, (c) case of three disks, (d) an example of *pinched* object with an arity  $A_P$  of 3.

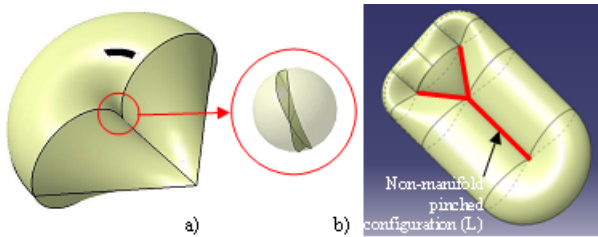


Fig. 4. a) An example of 'cross-cap'-type surface with its point neighborhood around the *pinched* line, b) A *pinched* configuration along a non-manifold structure.

two disconnected disks neighbourhood around point  $I_1$  (see Fig. 3(b)).

Then, introducing Figure 3c leads to the concept of arity,  $A_P$ , characterizing the number of disks connected to the *pinched* point  $I_1$ .

Up to now, the non-manifold objects  $\Sigma$  produced can be assigned two categories of orientation with a normal pointing either inward or outward since  $\Sigma$  still divides  $E^3$  into two distinct regions. Considering now a degenerated sphere with a non-manifold configuration set along a line, the result displayed at Figure 4a can be interpreted in two different ways as:

- $\Sigma$  a non-manifold *pinched* object embedded in  $E^3$ ,
- $\Sigma$  a non-orientable surface immersed in  $E^3$ , leading to an embedding with a self-intersection. This object is similar to the so-called 'cross-cap'.

As a common denominator, this non-manifold configuration is now defined by two disks or two 'cones' tangent to each other along the *pinched* line. This

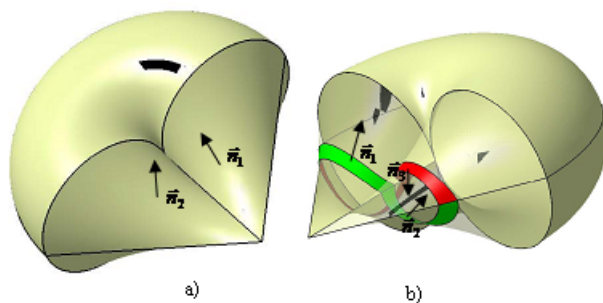


Fig. 5. The two different orientation schemes around the *pinched* line.

*tangent* line is part of the explicit self-intersection of  $\Sigma$ . At the opposite, the two objects differ from each other in term of orientation around the *pinched* line, this line being considered as an explicit self-intersection of the non-orientable object. Figure 5 illustrates the differences between the orientations around the *pinched* line in both cases. Figure 5a illustrates the transition  $\Theta_1$  for a non-manifold object defining a volume object. Figure 5b characterizes the transition  $\Theta_2$  for the 'cross-cap'.

Considering now Figure 5a, its transformation from a sphere  $\Sigma$  can be seen as a sequence of elementary operators combining shape deformations, merging operations along the self intersection line and edge collapse at the end of the line. As a result, the alternate sum of the Betti numbers is kept unchanged.

Figure 5b containing a 1-cycle of type Moebius strip increments the value of  $\beta_1$ . As a result, the transition function and the *pinched* entities entirely characterize the above set of objects.

Next, let us consider a configuration taking place along a simplicial 1-complex  $L$  (see Figure 4b) without 1-cycle. Applying the vertex and edge merging operators, it appears that the number of vertex and edge mergings equilibrate, showing that this configuration does not modify  $\beta_1$ . Hence, this object assigned with a transition function of type  $\Theta_1$  can be distinguished from the others using the topological description of the *pinched* area,  $L$ .

## 5.2 Degenerate torii

Starting now from the torus as reference shape, the classification addresses holes defined from two complementary 1-cycles. This reference shape exemplifies the transformation of shapes containing through holes defined with two 1-cycles, each one being associated with an orientable strip.

Degeneracies of torii  $D_j$  are studied through the degenerate configurations of their 1-cycles. Among them, degenerated 1-cycles of type  $\beta_{11}$  (see Figure 3a) lead to the *pinched* configuration and have already been studied. Then, degenerating 1-cycles of type  $\beta_{10}$  produces a configuration designated as *squeezed*. Two complementary aspects are addressed from the classification point of view:

- torus squeezed at point and orientation information,
- criterion about orientation to distinguish between *squeezed* torus and *pinched* sphere.

The *squeezed* configuration is illustrated with Figure 6a. The neighbourhood of  $I_2$  is identical to that of  $I_1$  (see Figure 3a) ; it is defined with two disks or two 'cones'. From the 1-cycles point of view, the torus can be transformed into the *squeezed* configuration through repeated edge collapse operations until the last stage of the transformation.

It should be noticed in this case that from a shape point of view the *squeezed* configuration still exhibits a through hole, i.e., the shrink configuration still looks like a ring, hence its distinction from the *pinched* one.

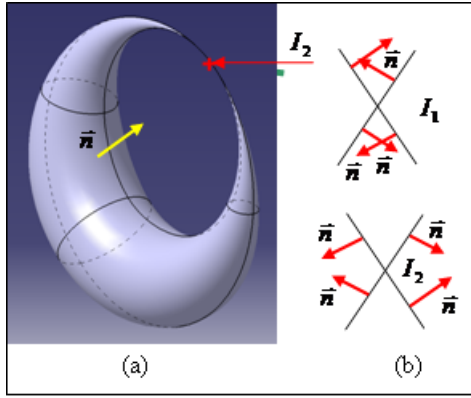


Fig. 6. (a) Transformation of a toroidal shape of  $D_j$  into a *squeezed* configuration at vertex  $I_2$  with a non-manifold intrinsic connection, (b) Configurations of normals around the points  $I_1$  and  $I_2$ .

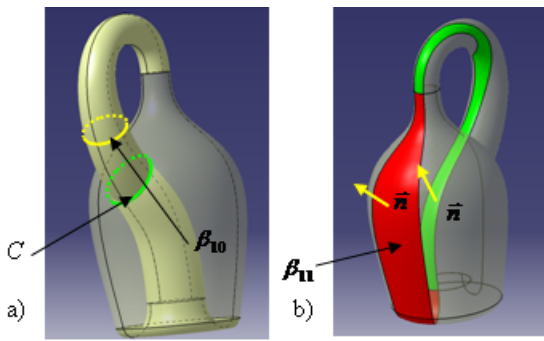


Fig. 7. Example of Klein bottle with its two reference 1-cycles,  $\beta_{10}$  and  $\beta_{11}$ .

As a result, these *pinched* sphere and *squeezed* torus contain the same number of 1-cycles, similar point neighbourhoods around  $I_1$  and  $I_2$ , respectively, and cannot be distinguished from each other. Because it is a point-based configuration, the transition function  $\Theta$  is not meaningful either.

Indeed, the orientation of the MC-component, which is applicable to these 2-manifolds without boundary, can be used to distinguish them from each other. Let us consider Figure 3a and Figure 6a evolving from their non-manifold configurations where the *pinched* sphere and *squeezed* torus are transformed into objects topologically equivalent to spheres. Figure 6b illustrates the orientation of normals around the points  $I_1$  and  $I_2$  when they share a common reference defined as the ‘exterior’ for both objects. Then, the distinction between *pinched* sphere and *squeezed* torus is possible as long as object orientation is uniformly set for orientable 2-manifolds, whether exterior or interior.

### 5.3 Degenerate Klein bottles

The Klein bottle characterizes non-orientable 2-manifold objects defined with two 1-cycles. One of them is defined from an orientable strip while the other one is a Moebius strip (see Figure 7). As a consequence of the definition of explicit self-intersection, the intersection curve  $C$  (see Figure 7) is intrinsically part of the

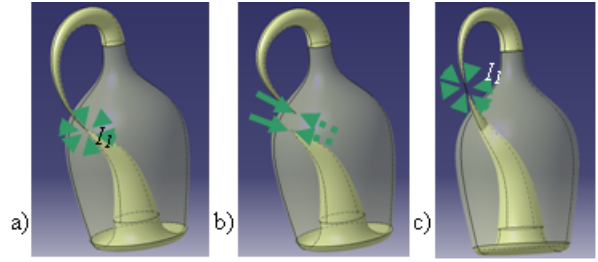


Fig. 8. Non-manifold configuration of a Klein bottle with a degenerated 1-cycle:  $\beta_{10}$ . a) represents the configuration where  $\beta_{10}$  degenerates at the self-intersection, b) depicts a possible evolution of the Klein bottle from configuration a) with *pinched* and *squeezed* configurations, c) configuration where  $\beta_{10}$  degenerates at an arbitrary location along the tubular shape of the Klein bottle.

simplicial complex  $\Sigma$  describing the Klein bottle. Hence, the MC-decomposition of a Klein bottle is no longer a unique MC-component but two MC-components  $D_1$  and  $D_2$  (see Figure 11).

Based on this reference object, non-manifold objects are generated through the following configurations:

- non-manifold configurations obtained with degenerated 1-cycles  $\beta_{10}$  located at different key positions along a 1-cycle  $\beta_{11}$ . Their effect produces *squeezed* and *pinched* configurations,
- non-manifold configurations obtained with degenerated 1-cycles  $\beta_{11}$  that produce the *twisted* configurations,
- analysis of the transition function  $\Theta$  in different non-manifold configurations.

In a first place, the 1-cycle  $\beta_{10}$  is degenerated at two key locations:

- the self-intersection curve  $C$ ,
- any location along  $\beta_{11}$  apart from  $C$ .

Figure 8a illustrates the effect of reducing the self-intersection curve  $C$  to a point. The corresponding configuration is called *squeezed* and *pinched* because it appears as a combination of these individual non-manifold configurations obtained from torii and spheres, respectively. The designation of this configuration is also justified by the fact that it can be obtained either from a sphere or a torus when applying to them the pinching and squeezing operations. It should be noticed that the result of this operation produces an orientable object because the *squeezed* and *pinched* configurations take place at vertices,  $\Theta$  is no longer meaningful and the MC-decomposition of this object now contains only one MC-component without boundary.

Point neighbourhood where the *squeezed* and *pinched* configurations take place differs from the degenerated sphere and torus cases. If the notion of ‘cone’ attached to non-manifold point can still be used, the *squeezed* and *pinched* configuration produces distinct ‘cones’ such that some of them are necessarily nested into others, which distinguishes this configuration from the previous ones. Figure 9a illustrates such a non-manifold configuration where ‘cones’ are nested into each other.

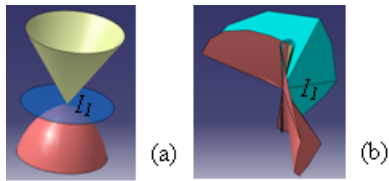


Fig. 9. a) General configuration where the neighborhood of  $I_1$  is defined by three cones, b) *twisted pinched* configuration in the neighbourhood of point  $I_1$ .

A second category of non-manifold configurations is produced when the 1-cycle  $\beta_{11}$  is degenerated. The effect is to preserve the tubular shape of the Klein bottle while some Moebius strip is reduced to a vertex. The corresponding object  $\Sigma$  is illustrated on Figure 10 where transparency helps understanding the shape of  $\Sigma$ . This non-manifold configuration is called a *twisted pinched* configuration because the singularity takes place at a point and its neighbourhood appears as twisted.

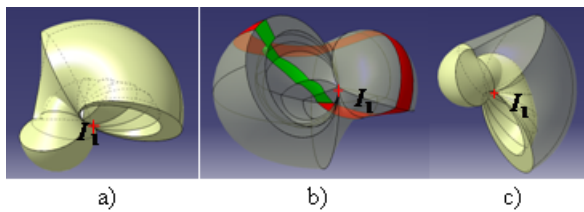


Fig. 10. Several views of the degenerated Klein bottle such that a non-orientable 1-cycle is reduced to a vertex. a), b) rotated views, c) transparency highlighting 'internal' structure of the non-manifold object.

Figure 9b describes the neighbourhood of *twisted pinched* point  $I_1$  showing that no separation process is applicable there, as observed when cutting along a closed path on a Moebius strip. Self-intersections with tangent 'cones' nested into others appears showing that further properties must be investigated there.

Because we consider an explicit self-intersection of the Klein bottle, the transition function is meaningful along  $C$ , which produces two possible relative orientations between  $D_1$  and  $D_2$  (see Figure 11a). If  $D_2$  has a normal pointing upward, this configuration can be taken to characterize the immersion of the Klein bottle. Now,

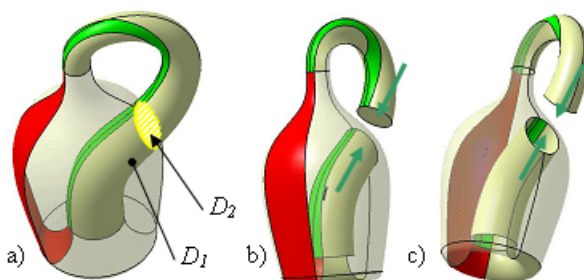


Fig. 11. a) Klein bottle with explicit self intersection as a torus with a stitched protrusion, b) a torus with a protrusion close to the stitching configuration, c) another view of the torus in b).

if  $D_2$  has a normal pointing downward, i.e., changing the relative orientation between  $D_1$  and  $D_2$ ,  $\Sigma$  can be interpreted as a torus with a protrusion stitched onto one of the 1-cycles defining its through hole. This is illustrated on Figure 11b and c where two views depict a configuration where the torus protrusion is about to be stitched onto its through hole.

## CONCLUSION

Degenerated objects have been distinguished from each other through their non-manifold singularities. For the sake of conciseness the analysis of the projective plane has not been detailed.

The proposed classification covers a wide range of configurations of non-manifold models that can be decomposed into manifold-connected 2-complexes and shows how it interacts with the object shape and the number of 1-cycles in the object. The transformations operated from the reference shapes is a contribution to a general purpose shape taxonomy covering all possible non-manifold singularities. It has been shown also how the concept of orientation interacts with the non-manifold singularities in the object. Further work is needed to study the general configuration of 1-cycles with an arbitrary twisting index. On the basis of the classification, data structures will be worked out to describe general purpose non-manifold models.

## REFERENCES

- [1] C.G. Armstrong, D.J. Monaghan, M.A. Price, H. Ou, and J. Lamont, Integrating CAE concepts with CAD geometry, In Engineering Computational Technology, pp. 75- 104, Saxe-Coburg Publications, 2002.
- [2] M. Rezayat, Midsurface abstraction from 3d solid models: General theory and application, CAD, 28(11), pp 905-915, 1996.
- [3] K. Weiler, The Radial Edge Structure: a Topological Representation for Non-manifold Geometric Boundary Modeling, Wozny, M.J., McLauhlin, H.W and Encarnação, J.L., editors, Geometric Modeling for CAD Applications, North-Holland, pp.3-36, 1988.
- [4] P. Lienhardt, Topological models for boundary representation: a comparison with n-dimensional generalized maps, CAD, Vol. 23(1), pp.59-82, Jan./Feb. 1991.
- [5] H. Masuda, Topological operators and Boolean operations for complex-based non-manifold geometric models, CAD, Vol. 25 (2), pp. 119- 129, February 1993.
- [6] J. A. Heisserman, A generalized Euler-Poincaré equation, ACM Symposium on Solid and Physical Model, Austin, Texas, 1991.
- [7] M. K. Agoston, Computer graphics and geometric modelling: Mathematics, Springer, 2005.
- [8] A. Hui, L. de Floriani, A two-level topological decomposition for non-manifold simplicial shapes, Solid and physical modeling conference 2007, Beijing, June 2007.
- [9] J-C. Léon, L. de Floriani, Contribution to a taxonomy of non-manifold models based on topological properties, ASME DETC CIE Conf., New-York, August 3-8th, 2008.

[10] H. Edelsbrunner, Geometry and Topology for Mesh Generation, Cambridge Univ. Press, 2001